Photon-number resolving detector based on a series array of superconducting nanowires

AIP | Applied Physics Letters

Photon-number resolving detector based on a series array of superconducting nanowires

S. Jahanmirinejad, G. Frucci, F. Mattioli, D. Sahin, A. Gaggero et al.

Citation: Appl. Phys. Lett. **101**, 072602 (2012); doi: 10.1063/1.4746248
View online: http://dx.doi.org/10.1063/1.4746248
View Table of Contents: http://apl.aip.org/resource/1/APPLAB/v101/i7
Published by the American Institute of Physics.

Related Articles

Bi-color near infrared thermoreflectometry: A method for true temperature field measurement
Rev. Sci. Instrum. 83, 124902 (2012)

Performance of the NIST goniocolorimeter with a broad-band source and multichannel charged coupled device based spectrometer
Rev. Sci. Instrum. 83, 093108 (2012)

The resolution estimation of wedge and strip anodes
Rev. Sci. Instrum. 83, 093107 (2012)

Note: Cryogenic microstripline-on-Kapton microwave interconnects
Rev. Sci. Instrum. 83, 086105 (2012)

Appearance potential spectroscopy with a photon counting detector and multiple scattering spectral interpretation
Rev. Sci. Instrum. 83, 083901 (2012)

Additional information on Appl. Phys. Lett.

Journal Homepage: http://apl.aip.org/
Journal Information: http://apl.aip.org/about/about_the_journal
Top downloads: http://apl.aip.org/features/most_downloaded
Information for Authors: http://apl.aip.org/authors

ADVERTISEMENT

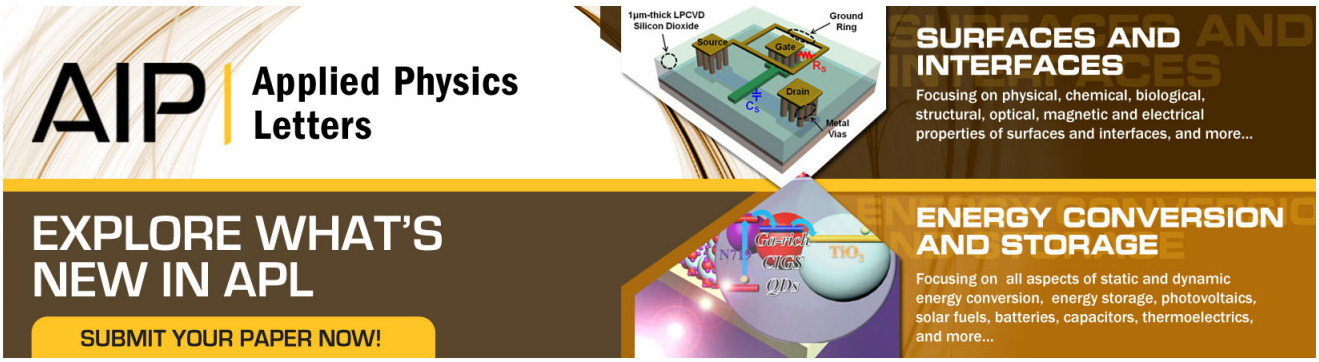

Photon-number resolving detector based on a series array of superconducting nanowires

S. Jahanmirinejad,[1,a)] G. Frucci,[1] F. Mattioli,[2] D. Sahin,[1] A. Gaggero,[2] R. Leoni,[2] and A. Fiore[1]
[1]*COBRA Research Institute, Eindhoven University of Technology, P.O. Box 513, 5600 MB Eindhoven, The Netherlands*
[2]*Istituto di Fotonica e Nanotecnologie, CNR, Via Cineto Romano 42, 00156 Roma, Italy*

(Received 22 March 2012; accepted 31 July 2012; published online 14 August 2012)

We present the experimental demonstration of a superconducting photon number resolving detector. It is based on the series connection of N superconducting nanowires, each connected in parallel to an integrated resistor. The device provides a single voltage readout, proportional to the number of photons detected in distinct nanowires. Clearly separated output levels corresponding to the detection of $n = 1–4$ photons are observed in a 4-element detector fabricated from an NbN film on GaAs substrate, with a single-photon system quantum efficiency of 2.6% at $\lambda = 1.3\,\mu$m. The series-nanowire structure is promising in view of its scalability to large photon numbers and high efficiencies. © *2012 American Institute of Physics*. [http://dx.doi.org/10.1063/1.4746248]

Conventional optical detectors generate an electrical signal proportional to the intensity of the incident light. However their sensitivity is limited by the electrical noise in the amplification circuit. On the other hand, single photon detectors (SPDs), which are extremely sensitive devices, usually show a strongly nonlinear response, i.e., their output signal level is independent of the number of photons that simultaneously hit the detector. The gap between these two detection regimes can be filled with a photon-number-resolving (PNR) detector, a device as sensitive as an SPD, and with a capability of determining the number of photons present in an incident pulse. Realization of PNR detectors would benefit many applications from linear optical quantum computing[1] to near-infrared spectroscopy.

In the last years, several detector technologies based on combining linear operation and single-photon sensitivity in one device have been demonstrated. However, in the telecommunication wavelength region, which is interesting for many applications, their performance has remained limited in terms of speed and dynamic range. For instance, transition-edge-sensors operated at sub-Kelvin temperatures show relatively slow response times,[2] while self-differencing InGaAs avalanche photodiodes (APDs) offer limited photon-number discrimination ability.[3] In another approach, PNR detection can be achieved by combining multiplexing techniques and SPDs. Time-multiplexed APDs have been reported, but with a necessarily reduced count rate due to the delay loops.[4,5] Frequency up-conversion combined with a silicon photomultiplier (SiPM) provides large dynamic PNR but with added noise due to up-conversion and cross-talk between the pixels, which requires detector calibration.[6] An array of nanowire superconducting single photon detectors (SSPDs) has been proposed to operate as a PNR detector based on spatial multiplexing, using either a separate readout for each element[7] or a parallel configuration with single output.[8] These implementations take advantage of the very high sensitivity, short dead time, and low timing jitter of SSPDs in the near-infrared range.[9] A detector geometry allowing a single readout of the photon number is particularly promising in view of simplicity of use and scalability to large photon numbers. However, the parallel nanowire detector[8] (PND) explored so far is limited in terms of dynamic range (maximum number of photons which can be detected in a pulse) and efficiency, due to the problem of current redistribution in the array after photon detection in one or more wires. The current redistribution issue can result in spurious switching of the wires which did not absorb a photon, generating false counts.[10] Avoiding this issue requires decreasing the number of elements in the array as well as limiting the bias current well below the critical current, which prevents reaching the highest efficiency in a conventional device with ~100 nm wide nanowires.

Recently, we have proposed[11] a device structure called series nanowire detector (SND), which is the electrical dual of PND and is designed to solve the current redistribution problem. It is based on the series connection of N nanowires, each connected in parallel to a resistor (R_P) as shown in Fig. 1(a). All the detecting sections are biased with the same bias current (I_B) close to the critical current (I_C). Upon absorption of a photon in one (firing) section, a large resistance develops in the wire, and the current is diverted into the parallel resistor producing a voltage pulse. If more photons are absorbed in distinct sections, the voltages produced across them are summed up at the output, resulting in a voltage proportional to the number of detected photons per pulse. Firing of a wire in the SND *reduces* the bias current in the other unfiring wires, as compared to the PND where the current in the unfiring wires is increased. This prevents the uncontrolled switching of the unfiring wires as it may happen in the PND if I_B is set very close to I_C. Therefore using the series configuration can result in higher QE and the possibility to scale to large photon numbers.[11] The device performance in terms of response amplitude and speed can be further optimized by means of a high-impedance preamplifier stage, easily realized using a high electron mobility transistor mounted close to the SND and operated cryogenically. In order to

a)Electronic mail: s.jahanmiri.nejad@tue.nl.

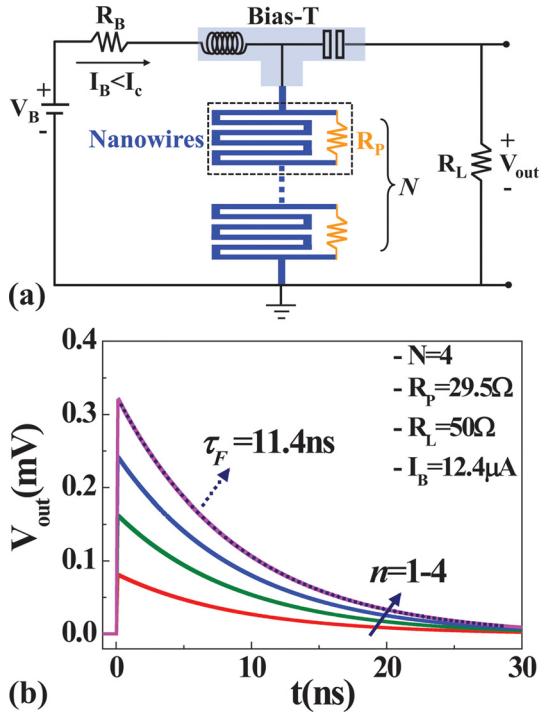

FIG. 1. (a) Schematics of the electrical circuit and the layout of an N-element SND structure. (b) Transient response of a 4-SND biased at $I_B = 0.99I_C$, simulated using the electrothermal model (Ref. 11).

illustrate the SND's photoresponse, Fig. 1(b) shows the simulated output voltage of a 4-element SND when $n = 1$–4 photons are detected in distinct elements. The simulation parameters are based on the model described in Ref. 11 and on the device parameters used in the experiment described below ($I_C = 12.5\,\mu A$, $I_B = 0.99I_C$, $R_P = 29.5\,\Omega$, $R_L = 50\,\Omega$, kinetic inductance $L_K = 100$ nH for each element). The relevant (1/e) time constant of the response exponential decay is approximately given by $\tau_F = N \times L_K/(N \times R_P \| R_L)$[11] and is calculated as $\tau_F = 11.4$ ns in this device. The recovery time of the device is expected to be $\sim 3 \times \tau_F$.

In this work, the fabrication and experimental demonstration of an SND with four detecting elements in series (4-SND) is reported, as a proof of principle. SNDs are fabricated from a 4.5 nm thick NbN film grown on GaAs substrate by reactive magnetron sputtering, at a nominal deposition temperature of 410 °C. This particular film exhibited a superconducting transition temperature of 9.5 K and a superconducting transition width of 0.7 K. To fabricate the SND structures, four nanolithography steps are carried out using field emission gun electron beam lithography (EBL) system with acceleration voltage of 100 kV. In the first step, Ti/Au (60 nm Au on 10 nm Ti) contact pads together with alignment markers are fabricated by lift-off using a polymethyl methacrylate (PMMA) stencil mask. This is followed by the second lithographic step to define the thin Ti/Au (20 nm Au on 5 nm Ti) pads used for the electrical contact of the resistors. In the third step, hydrogen silsesquioxane (HSQ) is used as an etch mask to pattern the meanders with RIE. In the last step the parallel resistors (40 nm thick AuPd film) are fabricated by lift-off via a PMMA stencil mask. Fig. 2 shows a scanning electron microscope (SEM) image of the fabricated SND with $N = 4$ detecting elements. The NbN nanowires are 100 nm wide, covering a total active area of $12 \times 12\,\mu m^2$ with a filling factor $f = 40\%$.

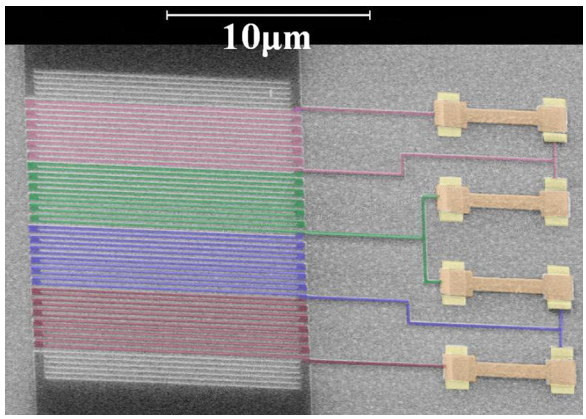

FIG. 2. SEM image of the 4-SND. The active wires, the parallel resistors, and their contact pads have been colored for clarity.

We performed the electro-optical characterization of the SND in a closed-cycle cryocooler with a base temperature of 1.18 K on the experimental plate and stability within 0.01 K. As it is schematically depicted in Fig. 1(a), the bias current is supplied through the DC port of a bias-T by a voltage source in series with a 10 Ω bias resistor. The current-voltage (I-V) characteristic of the device is displayed in Fig. 3. In the superconducting state, the parallel resistors are short circuited by the zero resistance of the wire, having no effect on the I-V. As soon as the bias current exceeds the critical current of a nanowire, a normal domain with finite resistance is formed across it, and a part of the bias current is pushed to the parallel resistance. Due to the effect of the parallel resistance, the typical relaxation oscillation regime and the hotspot plateau are not observed. In a section, when the entire length of a nanowire becomes normal, the resistance is the parallel equivalent of the nanowire normal resistances (estimated to be $R_{nanowire} \sim 70\,k\Omega$, from the measured normal resistance of test SSPD devices on the same chip) and R_P, which is very close to R_P. Following the transition of all the sections to the normal state, the device has a resistance equal to the sum of all parallel resistances. The reciprocal of the slope of the linear fit indicated in Fig. 3 corresponds to $4 \times R_P = 118\,\Omega$; hence, R_P is estimated to be 29.5 Ω.[12]

For the optical characterization, the light produced by a pulsed laser-diode with 50 ps pulse width, 1.3 μm wavelength, and 10 MHz repetition rate was coupled to the device

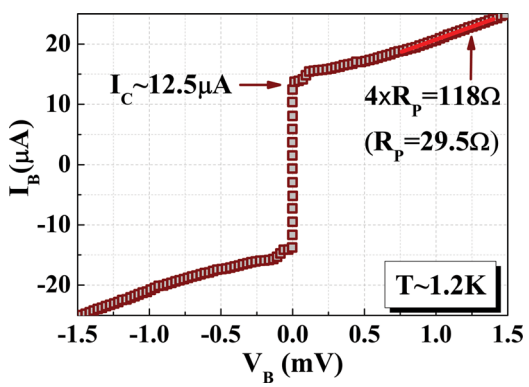

FIG. 3. IV characteristics of the 4-SND.

through a single-mode polarization maintaining lensed fiber with $1/e^2$ beam diameter of 5 μm mounted on XYZ piezo stages. The fiber connector key was oriented with the fast axis, which was aligned in a direction parallel to the nanowires. The output signal of the detector was collected at room temperature through the RF arm of the bias-T, amplified using a chain of wideband amplifiers and directed either to a 40-GHz bandwidth sampling oscilloscope or a 350-MHz counter for optical characterization.

To investigate the photon number resolving capability of the detector, the distribution of the output voltage pulses was measured using a sampling oscilloscope triggered with the laser-diode modulation signal. In order to couple the light equally to all sections of the SND, the beam was defocused to a larger spot diameter, estimated to be ~20 μm, achieving uniform illumination across the $12 \times 12\ \mu m^2$ area of the detector. Fig. 4(a) shows as an example the oscilloscope persistence map measured at $I_B = 8.3\ \mu A$ and average number of detected photons per pulse $\mu_{det} \approx 2.9$ (Ref. 13). Discrete voltage heights corresponding to the switching of 1 to 4 elements can be observed. The symmetric pulse shape, especially the slow rise time, as compared to the calculated response in Fig. 1(b), is ascribed to the effect of a low-pass filter (DC-80 MHz) used to remove the high frequency noise of the signal and to improve the visibility of the voltage peaks, which were discernible even without this low-pass filter (see supplementary material[21]). The inset in Fig. 4(a) shows the persistence trace without using the lowpass filter for a higher photon flux so that only the 4-photon detection is observed. The simulated output voltage when all of the four detection sections of SND fire is also plotted, showing good agreement with the experimental data. The minor discrepancies in the rise/fall times originate from the effect of the amplifier bandwidth which is not considered in the simulation. The related histogram for the recorded peak voltage levels is shown in Fig. 4(b), featuring a series of peaks broadened due to the presence of noise. The histogram can be fitted with a multiple-peak Gaussian distribution (solid light blue line) where each peak, corresponding to the switching of different number of elements in the SND, has a Gaussian distribution (gray dotted curves). The first peak which is entirely due to the electrical noise corresponds to the case when no photon was detected ("0"-level). The peaks at 12.5, 24.5, 37, and 50 mV correspond to the switching of 1, 2, 3, and 4 elements, respectively. The evenly spaced, clearly resolved peaks in the histogram show the photon-number-resolving functionality of the SND structure and confirm that conventional 50 Ω amplification is sufficient for the 4-SND to distinguish up to four detected photons per pulse. We observe an increase in the widths of the Gaussian peaks when the photon number is increased, which is an indication of an excess noise. The inset in Fig. 4(b) plots the measured excess noise, defined as $E_n = (\sigma_n^2 - \sigma_0^2)^{0.5}$, where σ_n and σ_0 are the standard deviations of the histogram peaks corresponding to n and 0 firing sections, respectively, as a function of n (see supplementary material for further discussion[21]).

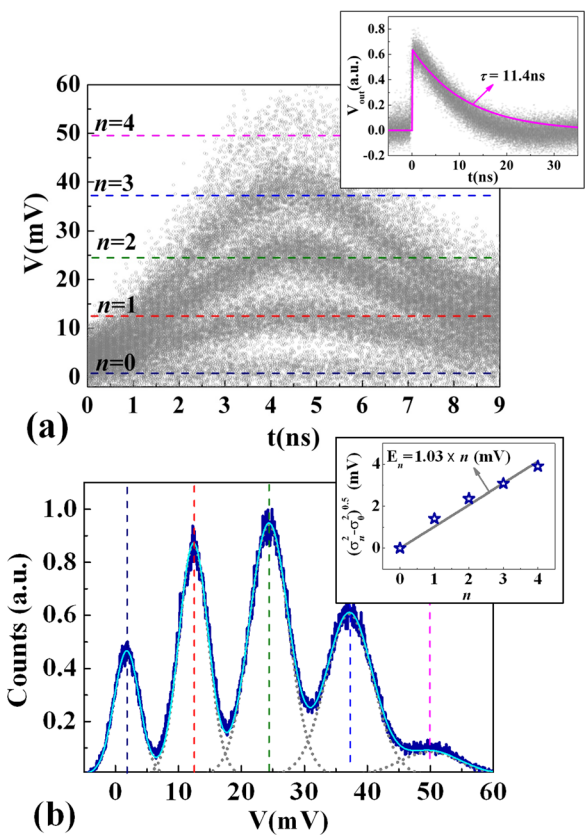

FIG. 4. (a) An oscilloscope persistence map at $\mu_{det} \approx 2.9$. Inset: A persistence trace related to detection of 4 photons per pulse together with the simulated output pulse. (b) Measured (dark blue) and fitted (light blue) pulse height distribution at $\mu_{det} \approx 2.9$, corresponding to the detection of up to 4 photons, along with the Gaussian fits (gray dotted line). The inset plots the excess noise of the SND, E_n, as a function of n.

In order to confirm that the four observed peaks are related to the detection of 1–4 photons, the photocount statistics were measured using a counter. The photoresponse of the SND was sent to the counter, and the photocounts were measured with the counter threshold level set to the midpoint between two of the detection levels observed in Fig. 4, for many different light powers. In this configuration, a count is measured when $n \geq n_{th}$ photons are detected. For illumination with a weak pulsed laser source such that $\mu_{det} \ll 1$, the count rate is expected to scale as $R(n_{th}, \mu_{inc}) \propto \mu_{det}^{n_{th}} = \eta^{n_{th}} \mu_{inc}^{n_{th}}$, where η is the quantum efficiency of each element and μ_{inc} is the average number of incident photons.[7] In Fig. 5 the measured count rates relative to one-, two-, three-, and four-photon absorption events are plotted as a function of μ_{inc} in log-log scale. The solid lines are the linear fits to the data with slopes

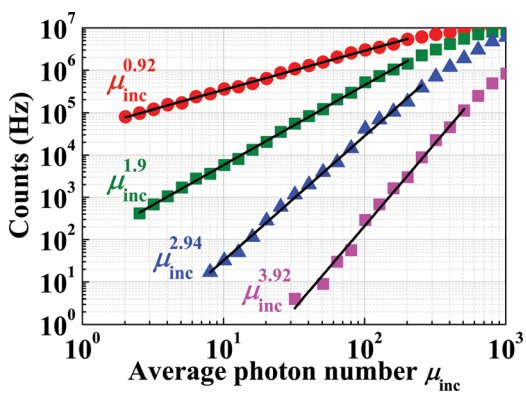

FIG. 5. Count rates measured at $I_B = 10\ \mu A$, relative to the $\geq 1, \geq 2, \geq 3$, and 4 photon detection events as a function of μ_{inc}.

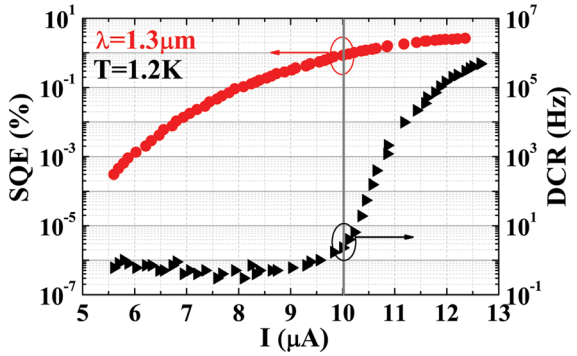

FIG. 6. Single-photon system quantum efficiency of the SND at $\lambda = 1.3\,\mu$m and dark count rate, as a function of the bias current.

very close to 1, 2, 3, and 4, which confirms that the detector responds to 1–4 photon detection events.

To characterize the SND in terms of efficiency, the single-photon system quantum efficiency (SQE) was measured under weak, well-focused central illumination such that only 1-photon detection event was observed. The value of SQE was obtained by dividing the number of photocounts (corrected for dark counts) by the average number of photons at the input of the cryostat. The result is plotted in Fig. 6 (left axis) as a function of bias current. The SQE attains its highest value of 2.6% at a bias current of $I_B = 12.4\,\mu$A ($0.99 \times I_C$) with the light polarized parallel to the wires. The calculated optical absorptance in a 4.5 nm thick NbN grating with 40% filling factor on GaAs substrate[14] is 9% under top illumination at $\lambda = 1.3\,\mu$m. Therefore, assuming a negligible fiber loss inside the cryostat, an intrinsic quantum efficiency (the ratio of detected to absorbed photons) of about 30% is derived for the device. The efficiency can be enhanced by improving the superconducting properties of the thin film, making narrower nanowires[15,16] and applying advanced optical structures such as optical cavities[14,17,18] or waveguides.[19] On the right axis of Fig. 6, the dark count rate (DCR) is presented as a function of the bias current, as measured by blocking the optical input to the cryostat and moving the fiber away from the device to suppress any spurious light input. A low background level of 1 Hz, due to electrical noise is measured at low bias currents, with a sharp increase for $I_B > 10\,\mu$A. At $I_B = 10\,\mu$A, a SQE of 1% and DCR of around 5 Hz are obtained.[20] The fact that the device could be operated at 99% of the I_C indicates the correct functionality of the shunted wire configuration, as predicted by our model[11] and therefore the possibility of reaching very high QEs. Furthermore, the timing jitter was measured at the leading edge of the voltage pulse, without lowpass filtering, using the sampling oscilloscope. After quadratically subtracting the jitter from the laser, the measured jitter of the detector, including the amplifying circuit, was 80 ps.

In conclusion, we have implemented a design for PNR detectors based on the series connection of N superconducting nanowires, each shunted with a resistance. The detection of $n = 1$–4 photons in the telecom wavelength range was demonstrated in a 4-element SND with maximum system quantum efficiency of 2.6% and recovery time constant in the 10 ns range. Scaling to large number of wires and integration of cavity or waveguide structures should enable efficient PNRs for linear detection in the few to few tens of photons range.

This research is supported by EU-FP7 projects QUANTIP (Project No. 244026) and Q-ESSENCE (Project No. 248095), the Dutch Technology Foundation STW, applied science division of NWO, the Technology Program of the Ministry of Economic Affairs (Project No. 10380), and NanoNextNL, a micro and nanotechnology program of the Dutch ministry of economic affairs, agriculture and innovation (EL&I) and 130 partners.

[1]P. Kok, W. Munro, K. Nemoto, T. Ralph, J. Dowling, and G. Milburn, Rev. Mod. Phys. **79**, 135–174 (2007).
[2]A. E. Lita, A. J. Miller, and S. W. Nam, Opt. Express **16**(5), 303 (2008).
[3]B. E. Kardynal, Z. L. Yuan, and A. J. Shields, Nat. Photonics **2**, 425 (2008).
[4]M. J. Fitch, B. C. Jacobs, T. B. Pittman, and J. D. Franson, Phys. Rev. A **68**, 043814 (2003).
[5]P. Eraerds, E. Pomarico, J. Zhang, B. Sanguinetti, R. Thew, and H. Zbinden, Rev. Sci. Instrum. **81**, 103105 (2010).
[6]E. Pomarico, B. Sanguinetti, R. Thew, and H. Zbinden, Opt. Express **18**(10), 10750 (2010).
[7]E. A. Dauler, A. J. Kerman, B. S. Robinson, J. K. W. Yang, G. G. B. Voronovc, S. A. Hamilton, and K. K. Berggren, J. Mod. Opt. **56**, 364 (2009).
[8]A. Divochiy, F. Marsili, D. Bitauld, A. Gaggero, R. Leoni, F. Mattioli, A. Korneev, V. Seleznev, N. Kaurova, O. Minaeva, G. Gol'tsman, K. G. Lagoudakis, M. Benkhaoul, F. Lévy, and A. Fiore, Nat. Photonics **2**, 302–306 (2008).
[9]G. Gol'tsman, O. Okunev, G. Chulkova, A. Lipatov, A. Semenov, K. Smirnov, B. Voronov, A. Dzardanov, C. Williams, and R. Sobolewski, Appl. Phys. Lett. **79**, 705 (2001).
[10]F. Marsili, D. Bitauld, A. Gaggero, S. Jahanmirinejad, R. Leoni, F. Mattioli, and A. Fiore, New J. Phys. **11**, 045022 (2009).
[11]S. Jahanmirinejad and A. Fiore, Opt. Express **20**(5), 5017–5028 (2012).
[12]Test resistors defined on each sample chip were measured to have a resistance of $\sim 30\,\Omega$ at $T = 4.2$ K, consistent with the value estimated from the slope of I-V.
[13]With the light intentionally defocused, we measured the single-photon system quantum efficiency at a very low photon flux by dividing the count rate to the number of photons at the input of the cryostat, resulting in a value of 0.076% at $I_B = 8.3\,\mu$A. In the case of Fig. 4, an average of 3800 photon/pulse was coupled at the input of cryostat fiber, which corresponds to 2.9 average detected photons per pulse.
[14]A. Gaggero, S. Jahanmirinejad, F. Marsili, F. Mattioli, R. Leoni, D. Bitauld, D. Sahin, G. J. Hamhuis, R. Nötzel, R. Sanjines, and A. Fiore, Appl. Phys. Lett. **97**, 151108 (2010).
[15]B. Baek, A. E. Lita, V. Verma, and S. W. Nam, Appl. Phys. Lett. **98**, 251105 (2011).
[16]F. Marsili, F. Najafi, E. Dauler, F. Bellei, X. Hu, R. Molnar, and K. K. Berggren, Nano Lett. **11**(5), 2048–2053 (2011).
[17]K. M. Rosfjord, J. K. W. Yang, E. A. Dauler, A. J. Kerman, V. Anant, B. M. Voronov, G. N. Gol'tsman, and K. K. Berggren, Opt. Express **14**, 527 (2006).
[18]B. Baek, J. A. Stern, and S. W. Nam, Appl. Phys. Lett. **95**, 191110 (2009).
[19]J. P. Sprengers, A. Gaggero, D. Sahin, S. Jahanmirinejad, G. Frucci, F. Mattioli, R. Leoni, J. Beetz, M. Lermer, M. Kamp, S. Höfling, R. Sanjines, and A. Fiore, Appl. Phys. Lett. **99**, 181110 (2011).
[20]The dark count measured with the fiber on top of the device was higher at low bias currents due to the effect of thermal radiation carried by the fiber. This effect can be improved by filtering out the unwanted radiation.
[21]See supplementary material at http://dx.doi.org/10.1063/1.4746248 for the discussion about the effect of lowpass filter and discussion on the observed excess noise.